


Research Article

Parameter Design in Carbonitriding of EN36, 16MnCr5, and AISI 4140 Steels Using Principal Component-Based Grey Incidence (PGI)

G. L. Arumparithy ¹, R. Adalarasan,² M. Santhanakumar,³ and Lijalem Mulugeta ⁴

¹Department of Mechanical Engineering, Saveetha Engineering College, Thandalam, Chennai, Tamil Nadu-602105, India

²Department of Mechanical Engineering, Saveetha School of Engineering, Saveetha Institute of Medical and Technical Sciences, Thandalam, Chennai, Tamil Nadu-602105, India

³Department of Mechanical Engineering, GRT Institute of Engineering and Technology, GRT Mahalakshmi Nagar, Tiruttani, Tiruvallur District, Tamil Nadu-631209, India

⁴Department of Mechanical Engineering, Institute of Technology, Hawassa University, Awassa, Ethiopia

Correspondence should be addressed to G. L. Arumparithy; arumparithygl14251425@gmail.com and Lijalem Mulugeta; lijalem@hu.edu.et

Received 5 March 2022; Accepted 4 April 2022; Published 13 April 2022

Academic Editor: V. Vijayan

Copyright © 2022 G. L. Arumparithy et al. This is an open access article distributed under the Creative Commons Attribution License, which permits unrestricted use, distribution, and reproduction in any medium, provided the original work is properly cited.

Case-hardening steels (EN36, 16MnCr5, and AISI 4140) are used in applications demanding good surface properties such as precision gears, shafts, and cam rollers. This study explores the formation of microcoatings to improve the surface characteristics of these steels using carbonitriding, which combines the merits of carburizing and nitriding to offer surfaces with enhanced hardness and wear resistance. Taguchi's L18 orthogonal array is used for conducting the carbonitriding trials with replications. The effects of various carbonitriding parameters like carbonitriding time, temperature, and flow rate of ammonia are studied on the treated surface characteristics (Vickers microhardness, diffusion depth, and wear loss). A novel integrated approach of principal component-based grey incidence (PGI) that combines the merits of both principal component analysis and grey incidence theory is effectively used to select the optimal carbonitriding inputs (material substrate AISI 4140, carbonitriding temperature -835°C , carbonitriding time-40 min, and flow rate of ammonia 0.4 lit/min). Microscopic images related to diffusion depths are also analyzed. This study offers the necessary guiding principles for obtaining the desired surface coating on EN36, 16MnCr5, and AISI 4140 steels.

1. Introduction

Gas carburizing is a surface treatment process employing an atmosphere of methane/propane at elevated temperatures along with a neutral carrier gas. It allows the induction of carbon into the surface of the specimen, which is finally quenched and tempered to finish the cycle [1]. The carburizing time and furnace temperature influence the Vickers microhardness and sliding wear behavior of carburized steels [2]. Carbonitriding is a modified version of gas carburizing involving the diffusion of carbon and nitrogen into the steel surface while maintaining the ductility of the core. The process of carbonitriding usually concludes with an oil/

brine quench, hence producing wear-resistant surfaces with reasonably good fatigue strength in an economical way [3]. The principle of carbonitriding involves heating the steel component in a sealed enclosure into its austenitic range, ensuring the required phase change and allowing the diffusion of carbon and nitrogen from an appropriate atmosphere [3]. Within a gas carburizing enclosure, ammonia dissociates to produce nascent nitrogen, which can easily diffuse along with carbon atoms into the surface of the specimen. The hardness of the substrate core is also maintained at higher temperatures because of nitrogen addition. Higher case depths and penetration rates are obtained using carbonitriding compared to nitrocarburizing

and gas carburizing. However, time and resource constraints determine the diffusion limits [4]. The hardenability of a carbonitrided case was generally better than a gas-carburized case as the cooling rate of steel was lowered by nitrogen addition. Though the effects of carbonitriding and cyaniding were similar, the disposal of cyanide wastes poses a significant problem in the process of cyaniding [5].

The surface characteristics of the carbonitrided case are influenced by the process inputs like carbonitriding time, temperature, furnace atmosphere, and type of substrate. However, the rate of nitrogen diffusion requires good control of the furnace atmosphere. Since the addition of more ammonia has a dilution effect in the carburizing atmosphere, controlling the flow rate of ammonia becomes essential for obtaining a good carbonitrided surface. The case and core microstructures were easily distinguishable in the carbonitrided specimen at a lower furnace temperature. The higher temperature poses difficulty in controlling the nitrogen addition into the surface of the specimen [6]. The final finishing operations may not be required in a carbonitrided specimen as relatively less severe quenching and lower temperature result in a reduced distortion of the workpiece. However, the process of nitrocarburizing had produced a lesser value of residual compressive stress compared to carbonitriding in the case of SAE 1010 steel [7]. The economy of the process could be best understood with less expensive carbonitrided steels offering surface characteristics similar to that of costly alloy steels subjected to gas carburizing. Carbonitriding of tool steel with a shorter processing time was found to improve its mechanical properties similar to that of chromium AISI H11 steel [8]. Better microhardness was observed in carbonitrided chrome-manganese steel compared to the effects of laser shock peening performed on the same substrate [9]. Considerable improvement in microhardness of carbonitrided steels could be correlated with the thickness of surface coating [10]. Nitrogen-rich case with a good fraction of nitrides was observed in carbonitriding of chrome alloy steels at 1173 K under NH₃ and CO-H₂ atmosphere [11]. Low-temperature nitriding of AISI 4140 steel could produce a significant increase in surface microhardness and a considerable reduction in wear loss [12].

The application of the Taguchi method in carbonitriding of AISI 1022 tapping screws had revealed the contribution of various process parameters like carbonitriding time, temperature, and furnace atmosphere in establishing the desired surface characteristics [13]. The Taguchi-grey method using the L₉ orthogonal array was used to optimize the process parameters in the surface treatment of AISI 1015 steel, and the grey relational grade was employed as the performance index [14]. Selection of proper levels of carbonitriding inputs is of utmost essential in obtaining the steel surfaces with desired properties including surface hardness, wear loss, and diffusion depth. Modeling using response surface methodology and generation of response surface plots and variance analysis were available in the literature to study the relationship between process variables and responses in various fields of engineering [15, 16]. Genetic algorithms could outperform techniques like neural networks, fuzzy logic, and

simulated annealing in modeling and optimization. The ability of response surface methodology in the irregular regions of experimental trials was questionable, while the setting of parameters in the genetic algorithm was complex [17]. Further tuning fuzzy logic to the dynamics of a process like carbonitriding was not an easy task. Grey relational analysis or an integrated approach of grey theory with desirability analysis was observed to be effective in selecting the optimal parameters for good surface characteristics [18, 19]. Grey relational grade matrix applied to Taguchi design was effective in identifying the optimal condition [20]. Principal component analysis (PCA) is an eigenvalue-based multivariate data analysis, which could perform better than Fourier transforms and factor analysis by considering the effects of variance in the data. PCA was successfully applied in various manufacturing scenarios in its genuine version or in hybrid forms after proper integration with established techniques [21, 22].

An extensive amount of literature was found on the surface treatment of various alloys using boronizing, carburizing, nitriding, and chromizing. However, limited work was observed in a combined process like carbonitriding, which pools the merits of both carburizing and nitriding. Further application of carbonitriding on case-hardening steels like EN36, 16MnCr5, and AISI 4140 employed in precision gears, shafts, and cam rollers was limited in the literature. Though PCA and theory of grey incidence were individually applied in various fields, an integrated approach of principal component-based grey incidence (PGI), combining the advantages of both methods to obtain optimal carbonitriding inputs, is scarce in the literature. Hence, an attempt has been made for parameter design in carbonitriding of case-hardening steels by applying the PGI method.

2. Surface Treatment Experimentation

2.1. Substrates and Heat Treatment Furnace. The case-hardening steels like EN36, 16MnCr5, and AISI 4140 possess high strength and deep hardening characteristics with a tough interior. This permits their applications in precision gears, shafts, rolled plates, strips, cam rollers, screws, levers, etc. Furthermore, the creep-resisting characteristics of these classes of steels are good at higher temperatures and can sustain their mechanical properties even after long exposures to elevated temperatures [23]. These case-hardening steels are procured in the form of circular rods of a diameter of 22 mm. The acquired rods of three different substrates (EN36, 16MnCr5, and AISI 4140 steel) are milled and finished to 15 mm square rods before subjecting them for carbonitriding. Required lengths of rods were cut and cleaned with acetone to remove the dirt and lubricants on the surface before treating them in the furnace. The carbonitriding furnace (Figure 1) rated at 30 kWh was used to treat the surface of three different substrates. It employs a Nikrothal® nickel chromium heating element capable of producing a peak temperature of 1120°C in the coils. The retort of the furnace is made of iron-chromium-aluminum alloy, a high-temperature construction material that can



FIGURE 1: Furnace displaying the heating element.

resist creep better than stainless steel grade 310 retorts. The temperature of the specimen was read by using a thermocouple (K-type) enclosed in the ceramic tube with the desired accuracy of $\pm 5^{\circ}\text{C}$. The required atmosphere was ensured inside the treating furnace with a carbon-bearing gas (CO_2) and arrangement to supply ammonia (NH_3) at the required flow rates. The surface-treated samples were oil quenched to room temperature to finish the process of carbonitriding.

2.2. Experimental Design and Testing. A standard diamond cutter in the machine shop was used to cut samples of different substrates into lengths of 40 mm. Carbonitriding is a safe and simple process handling zero salts and requiring lesser cleaning. The important parameters controlling the surface characteristics of a treated specimen were identified from the available scientific literature [1, 3, 4, 7, 8]. Preliminary carbonitriding trials on EN36, 16MnCr5, and AISI 4140 steels were observed to produce better surface characteristics than carburizing and through hardening performed with industrial expertise on the same material substrates. Few samples from preliminary surface treatment studies are shown in Figure 2. Pilot carbonitriding trials were performed with various dominant parameters like carbonitriding time, carbonitriding temperature, and flow rate of ammonia on the three different substrate materials. The range of carbonitriding inputs delivering a reasonably good improvement in surface characteristics was chosen for study. The different levels of carbonitriding inputs chosen for experimentation are shown in Table 1. Taguchi's L18 orthogonal array design was used to perform the carbonitriding trials with replications. Considering the number of parameters (four) and the number of levels (three), a L18 orthogonal array was selected instead of a L9 orthogonal



FIGURE 2: Samples from pilot surface treatments including carburizing and through hardening.

array for better resolution. However, the experimental trials were not performed in an exact sequence of parameter combinations to minimize the extraneous effects [17].

An atmosphere of CO_2 and desired flow rate of ammonia were ensured at a set temperature and time in the furnace. Ammonia cracks on the specimen surface to produce nascent nitrogen, which diffuses into the surface heated to the austenitic range, along with carbon from the carrier gas. The zirconia type oxygen sensor along with a two-loop controller was used to automatically maintain the value of carbon potential in the range of 0.9 to 1.0. The treated specimen was quenched in SAE-40 oil maintained at 100°C for 5 min to prevent distortion and finish off the process sequence [23]. The surface quality characteristics observed include Vickers microhardness (HV), diffusion depth (DD), and wear loss (WL). Few samples of different material substrates subjected to carbonitriding trials can be seen in Figure 3.

The surface hardness (HV) of the treated surfaces was measured using a Vickers microhardness tester (model: VH1150, Wilson Wolpert, Germany make) with a load range capability of 10 g to 1 Kg. Vickers hardness testing was performed by following the ASTM B487-2002 standard (load- 100 g, t- 10 s) using a diamond indenter. The averaged hardness (HV @ 0.1 Kg) from three different places on the treated surface was taken for further analysis. Sliding occurring between a rotating disc and static pin in a pin on disc wear test rig (Saini make SSI-114) was used to measure the wear loss. The setup was furnished with a preset timer and normal load-applying capabilities in the range of 5 N to 30 N. Initially, the sliding surface was cleaned to remove quenching oil and a wear test was performed at a load of 10 N using alumina as abrasive. The sliding velocity was maintained at 1.5 m/s for a time period of 600 s. A digital weighing balance (Kerro make, P7 model) with a maximum weighing capability of 220 g and weighing accuracy of 0.1 mg was used to compare the weight of the specimen before and after the

TABLE 1: Levels of carbonitriding inputs.

Inputs	Symbol	Units	Levels of parameters		
			Level 1	Level 2	Level 3
Material substrate	A	—	EN36	16MnCr5	AISI 4140
Carbonitriding temperature	B	°C	800	850	870
Carbonitriding time	C	min	30	40	50
Flow rate of ammonia	D	lit/min	0.3	0.4	0.5

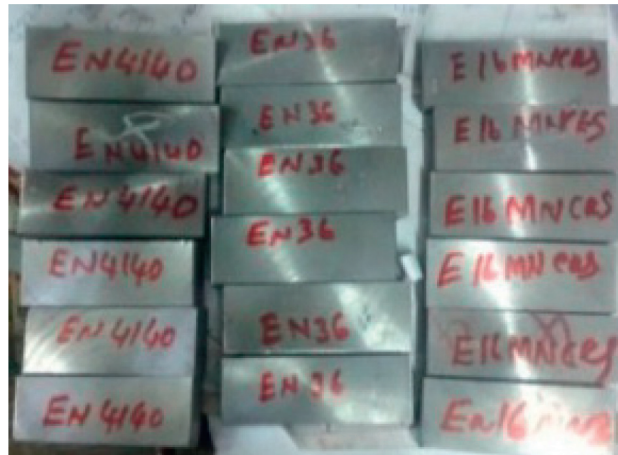


FIGURE 3: Samples of different material substrates subjected to carbonitriding.

wear test. For observing the diffusion depth, a section of the specimen was polished in silica suspension and subjected to buffing. It was molded in bakelite and etched with 2% Nital for 30 s. The field emission scanning electron microscope (FESEM) images to study the diffusion depths were taken from scanning electron microscope (Carl Zeiss- MA15/EVO 18) with a resolution of 2.5 nm and an image control processor. By following the ASTM B487-2002 standard, images were taken from specimens in a low-vacuum mode at 20 kV, properly controlled by a 5-axis motor. The equipment used for testing and few samples prepared for the micro-examination are shown in Figure 4.

2.3. Experimental Observations. The diffusion depths attained in the substrate material were a function of carbonitriding temperature and surface treatment time. However, the passage of time during which the substrate was at the actual desired furnace temperature along with the metallurgical effect of heating-up time was not explored in scientific literature. The changes in nitrogen diffusing in its nascent form into the substrate surface were more only if ammonia cracks at the surface, which otherwise will result in the formation of molecular nitrogen [3]. This offers the necessary space for studies related to the rate of nitrogen pickup and state-of-the-art monitoring of temperature during heating time inside the furnace atmosphere. The quality characteristics (HV, DD, and WL) observed during the surface treatment with different combinations of inputs are presented in Table 2.

3. Principal Component-Based Grey Incidence (PGI)

The simultaneous optimization of several responses from carbonitriding is an effective technique for offline quality control [17]. Simultaneous optimization of multiple responses poses a significant level of difficulty, requiring more experimental trials and compound analysis. Hence, an attempt has been made to integrate the merits of eigenvector analysis and grey incidence theory in a novel principal component-based grey incidence (PGI) methodology. The various steps in the PGI technique are presented in two stages.

3.1. Stage I: Principal Component Analysis. The application of principal components in analyzing the responses of a manufacturing process was apprehended in existing literature [20]. Stage I is focused on the orthogonal transformation of observed responses into linearly uncorrelated principal components, which use the *signal-to-noise ratio* (S/N ratio) as an input measure. The correlated coefficient array leads to principal components, which are fed as inputs to the theory of grey incidence in the following steps.

Step 1. Calculation of the S/N ratio (η_{ij}) for the outputs (y_{ij}) of carbonitriding process using the relevant equation. The step involves following two characteristics (*smaller-the-better* and *larger-the-better*) and obtaining the corresponding S/N ratio values using equations (1) and (2), with “n” indicating the number of replications.

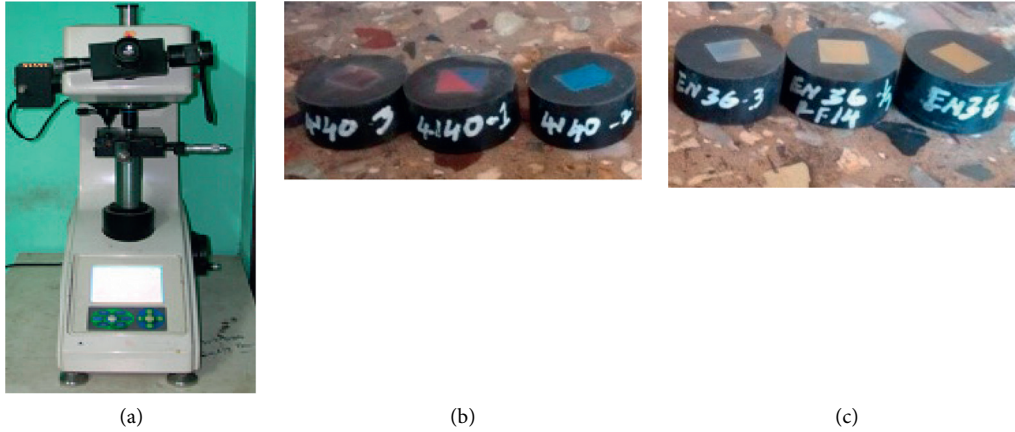


FIGURE 4: (a) Vickers hardness tester and (b) samples in bakelite mold for microexamination.

TABLE 2: Carbonitriding parameter combinations and the observed responses.

Order of trials		Surface treatment inputs				Responses					
Actual	Random	A	B	C	D	HV @ 0.1 Kg		DD (μm)		WL (gm)	
1	7	EN36	800	30	0.3	532	533	77	78	0.0171	0.0169
2	3	EN36	835	40	0.4	549	551	91	93	0.0145	0.0143
3	4	EN36	870	50	0.5	564	567	94	93	0.0140	0.0142
4	2	16MnCr5	800	30	0.4	604	606	100	100	0.0123	0.0121
5	17	16MnCr5	835	40	0.5	685	685	108	109	0.0132	0.0133
6	18	16MnCr5	870	50	0.3	612	607	104	102	0.0136	0.0135
7	1	AISI4140	800	40	0.3	643	639	92	90	0.0145	0.0146
8	16	AISI4140	835	50	0.4	718	720	110	111	0.0099	0.0105
9	12	AISI4140	870	30	0.5	684	680	103	102	0.0115	0.0115
10	14	EN36	800	50	0.5	503	503	101	100	0.0191	0.0190
11	6	EN36	835	30	0.3	535	540	95	92	0.0162	0.0164
12	9	EN36	870	40	0.4	688	686	117	118	0.0122	0.0120
13	10	16MnCr5	800	40	0.5	624	619	101	100	0.0163	0.0165
14	11	16MnCr5	835	50	0.3	706	705	96	97	0.0148	0.0149
15	13	16MnCr5	870	30	0.4	692	687	94	95	0.0126	0.0125
16	8	AISI4140	800	50	0.4	635	638	97	96	0.0154	0.0156
17	5	AISI4140	835	30	0.5	678	676	106	108	0.0137	0.0136
18	15	AISI4140	870	40	0.3	682	680	109	110	0.0164	0.0163

Smaller-the-better response to get a minimal value of response

$$\frac{S}{N} \text{Ratio}(\eta) = -10 \log_{10} \left(\frac{1}{n} \sum_{i=1}^n y_{ij}^2 \right) \quad (1)$$

Larger-the-better response to get a maximum value of response

$$\frac{S}{N} \text{Ratio}(\eta) = -10 \log_{10} \left(\frac{1}{n} \sum_{i=1}^n \frac{1}{y_{ij}^2} \right) \quad (2)$$

Step 2. Data normalization is an essential step to bring down the variability among S/N ratios of various outputs [21]. It is performed as a part of preprocessing by using equation (3), to bring the transformation of S/N ratio values in the range 0 Z_{ij} 1, with “ m ” being the number of trials.

$$Z_{ij} = \frac{y_{ij} - \max(y_{ij}, i = 1, 2, \dots, m)}{\max(y_{ij}, i = 1, 2, \dots, m) - \min(y_{ij}, i = 1, 2, \dots, m)} \quad (3)$$

Step 3. Formation of a multiquality characteristic array (z_i^j) with the normalized S/N ratio values [20], with “ i ” varying from 1 to m and “ j ” varying from 1 to n .

$$Z_i^j = \begin{bmatrix} z_1^1 & \dots & z_n^1 \\ \vdots & \ddots & \vdots \\ z_1^m & \dots & z_n^m \end{bmatrix} \quad (4)$$

Step 4. Formation of a correlation coefficient array (R_{ij}) using equation (4), with $\text{Cov}(z_i(j), z_i(l))$ as the covariance of sequences $z_i(j)$ and $z_i(l)$, $\sigma_{(z_i)(j)}$ as standard deviation of

the sequence $z_i(j)$ and $\sigma_{(z_i)(l)}$ as deviation of the sequence $z_i(l)$.

$$R_{jl} = \left(\frac{\text{Cov}(z_i(j), z_i(l))}{\sigma_{(z_i)(j)} \times \sigma_{(z_i)(l)}} \right). \quad (5)$$

Step 5. Determination of eigenvalues and eigenvectors [20] from the correlation coefficient array using equation (5), with λ_k being the eigenvalue and $V_{ik} = [a_{k1}, a_{k2}, \dots, a_{kn}]^T$ as the eigenvector corresponding to eigenvalue λ_k .

$$(R - \lambda_k I_m) V_{ik} = 0. \quad (6)$$

Step 6. Calculation of the uncorrelated principal components with “ P_{m1} ” being the first principal component, “ P_{m2} ” as the second principal component, and so on using equation (6). The generated values are normalized further before casting the grey incidence on principal components.

$$P_{mk} = \sum_{i=1}^n z_m(i) \cdot V_{ik}. \quad (7)$$

3.2. Stage II: Grey Incidence Theory. Stage II predominantly deals with the formation of desired performance index (DPI) using the grey incidence theory. DPI is used as a single-quality characteristic that encompasses all the outputs observed during the study. Hence, it leads to the optimal combination of carbonitriding parameters in the following steps.

Step 7. Computation of the grey incidence coefficient (Υ) values from the normalized principal components obtained in “Step 6” using equation (7). This is performed to present the linkage and for offering a comparison between the best and actual normalized experimental results [21].

$$\Upsilon[P_0(k), P_i(k)] = \frac{\Delta_{\min} + \xi \Delta_{\max}}{\Delta_{oj}(k) + \xi \Delta_{\max}}, \quad (8)$$

$\Delta_{oj} = P_0(k) - P_i(k)$ is the absolute difference between “ $P_0(i)$ ” (reference sequence) and $P_j(i)$ (specific comparison sequence), $\Delta_{\min} = \min P_0(k) - P_i(k)$ is the smallest value of $P_j(i)$, $\Delta_{\max} = \max P_0(k) - P_i(k)$ is the largest value of $P_j(i)$, and ξ is the distinctive coefficient with a value of 0.33, ensuring an equal weightage for all the outputs.

Step 8. Computation of the desired performance index (DPI) from the calculated values of grey incidence coefficients of each response using equation (8). The proportion of explained variances (PEVs) is considered as the weights for corresponding grey incidence coefficients.

$$DPI_i = \sum_{j=1}^n \left(\Upsilon_{ij} \times \frac{\lambda_j}{\sum_{k=1}^n \lambda_k} \right). \quad (9)$$

Step 9. Identification of the optimal level of carbonitriding parameters based on DPI. The main effects (ϵ_i) of the process variables and predicted S/N ratio ($\bar{\eta}$) at the selected optimal levels of inputs are calculated using equations (9) and (10), respectively. The best level of input is selected as the one with the largest value of DPI.

$$\epsilon_i = \max(DPI_{ij}) - \min(DPI_{ij}), \quad (10)$$

$$\bar{\eta} = \eta_m + \sum_{i=1}^f (\bar{\eta}_i - \eta_m), \quad (11)$$

where η_m and f represent the average S/N ratio and number of control factors, respectively.

Step 10. Prediction of factor significance and their contribution to arriving at responses by analyzing the variance (ANOVA) on DPI values [13].

Step 11. Validation of the integrated methodology of PGI through confirmation experiments carried out at the optimal levels of carbonitriding parameters.

4. Results and Discussion

All the material substrates were subjected to the metallurgical surface treatment of carbonitriding using the combination of inputs prescribed by the L18 orthogonal array. The responses obtained were subjected to further analysis.

4.1. Preprocessing and Normalization of S/N Ratio. The ratio of required signal (process average) to noise (standard deviation) measured as the S/N ratio was calculated for various quality characteristics using the appropriate equations (equations (1) and (2)). The S/N ratio used as an initial index is the reciprocal of the coefficient of variation that measures the relative dispersion of data. The surface hardness and diffusion depth were treated as “larger-the-better,” while wear loss was the “smaller-the-better” quality characteristic with desired values of 1 (maximum) and 0 (minimum), respectively. Aligning the data toward a normal distribution makes the analysis easier by increasing the comparability of process variables. The experimental data were converted in the range of 0 to 1 by linear normalization, which was essentially a process of scaling. Equation (3) was used to complete the initial step of data preprocessing. The pre-processed data are presented in Table 3.

4.2. Grey Incidence Coefficient and Desired Performance Index (DPI). The linear combination of each individual response was used to present the structure of variance-covariance better. A correlation coefficient array was formed by considering the normalized values of the S/N ratio of responses. Eigenvalues, eigenvectors, and principal components were calculated using equations (5) and (6), and the uncorrelated principal components were aligned downward by considering variance. This step effectively converts the correlated variables (observations) into uncorrelated ones

TABLE 3: Preprocessed data.

Trial	S/N ratio			Normalized S/N ratio		
	HV	DD	WL	HV	DD	WL
1	56.035	37.745	37.760	0.266	0.000	0.341
2	56.157	39.268	38.145	0.347	0.415	0.411
3	56.278	39.405	37.393	0.427	0.452	0.273
4	55.635	39.979	38.230	0.000	0.608	0.427
5	56.720	40.705	38.358	0.721	0.806	0.450
6	56.430	40.252	37.965	0.528	0.682	0.378
7	56.178	39.158	38.786	0.360	0.385	0.529
8	57.141	40.866	40.685	1.000	0.850	0.878
9	56.726	40.178	39.642	0.725	0.662	0.686
10	56.137	40.029	35.907	0.333	0.622	0.000
11	56.110	39.403	37.052	0.315	0.451	0.210
12	56.469	41.418	38.244	0.554	1.000	0.430
13	55.924	40.054	37.523	0.192	0.629	0.297
14	56.682	39.722	36.688	0.695	0.538	0.144
15	55.904	39.486	38.800	0.178	0.474	0.532
16	56.055	39.696	36.227	0.279	0.531	0.059
17	56.358	40.588	37.316	0.480	0.774	0.259
18	56.846	40.775	41.349	0.804	0.825	1.000

(principal components), hence eliminating an independent component analysis. Eigenvalues were 1.820, 0.652, and 0.364 for the three principal components with the proportion of explained variation (PEV) values of 0.643, 0.229, and 0.128. Table 4 shows the values of normalized principal components and DPI.

The normalized principal components were used to form a single reference entity (DPI) for the carbonitriding responses bearing different quality characteristics. The grey incidence coefficients form the basis for the calculation of the DPI values. Hence, the integrated methodology of PGI had effectively reduced a multiresponse problem into the optimization of a single characteristic, permitting simultaneous optimization. The DPI values were used to study the effects of carbonitriding inputs on the quality characteristics. The DPI values are plotted for various experimental trials (Figure 5). These single representatives assist in giving a picture of the overall effects of defined parameter combinations on the observed responses. Their contribution was realized in the conversion of a multiresponse optimization problem into the optimization of a single response. A higher value of DPI defines better surface properties irrespective of the nature of responses, which require maximization or minimization or a user-defined target value. The DPI value for the trial number 8 was observed to be the highest, indicating the closeness of experimental parameters to a near-optimal one.

4.3. Parameter Effects on Normalized S/N Ratio and Analysis of Variance. The parameter effects on DPI values were found out, and the optimal levels of carbonitriding inputs were selected based on max-min criteria (Figure 6). The optimal levels of inputs for better surface hardness, diffusion depth, and wear loss were chosen as follows: material substrate- AISI 4140 steel, carbonitriding time- 40 min, carbonitriding temperature -835°C , and flow rate of

ammonia- 0.4 lit/min. Analysis of variance was performed on DPI values to find the contribution of each parameter toward the observed responses. The carbonitriding temperature (30.9%) and carbonitriding time (22%) were observed to influence the responses to a larger extent compared to the other parameters (Table 5), as they influence the diffusion of carbon and nitrogen into the surface of the specimen.

The effects of various parameters were studied on the responses in terms of normalized S/N ratio. Among the various material substrates, AISI 4140 steel was observed to have larger diffusion depths (Figure 7(a)). Hence, AISI 4140 steel shows a good degree of surface hardening compared to EN36 and 16MnCr5 substrates. The diffusion depth was more at higher temperatures within the test range as elevated temperature improves the carbon potential inside the furnace atmosphere, permitting the diffusion of carbon atoms to the interstitial spaces (Figure 7(b)). Carbonitriding was a process characterized by a shorter processing time compared to carburizing [3]. A moderate processing time becomes important within the test range for better diffusion depths (Figure 7(c)). An increased carbonitriding time beyond a certain level causes carbon deposit from enriching gas, hence generating soft spots over the surface creating problems with cleaning as well [3]. An increase in the flow rate of ammonia inside the furnace atmosphere increases the chances of nitrogen diffusion; however, diffusion depths were improved only if nascent nitrogen was available near the specimen surface. Beyond a flow rate of 0.4 lit/min, diffusion depth improvements were meager (Figure 7(d)), which could be attributed to the formation of molecular nitrogen rather than nascent nitrogen having a higher diffusion capability.

The interstitial diffusion of nitrogen and carbon atoms on the treated steel surface forms iron carbides and iron nitrides, which offer the required degree of resistance to the slip of crystals on a microscopic scale, hence enhancing the hardness. The surface microhardness was observed to be larger on AISI 4140 steel subjected to carbonitriding compared to EN36 and 16MnCr5 substrates (Figure 7(a)). The amount of retained austenite was relatively higher due to nitrogen acting as an austenite stabilizer during carbonitriding. Furthermore, it lowers the transformation temperature of austenite resulting in the increased possibility of fine martensitic transformation [24]. Hence, for similar amounts of carbon in the substrate, carbonitriding increases the hardenability of steels. The retained austenite gives good workability to the material, which was highly desired in precision gears for noiseless applications [3, 22]. At higher carbonitriding temperature, the diffusion of nitrogen acting as an austenite stabilizer was lower, resulting in a relatively low surface hardness (Figure 7(b)). Further soft deposit of carbon was known to decrease surface hardness at higher temperature ranges. Though carbonitriding time increases the surface hardness, only meager improvements were observed beyond 40 min (Figure 7(c)). This could be due to a reduction in the diffusion of nascent nitrogen and carbon into the surface.

The wear loss was found to be better in carbonitrided AISI 4140 steel compared to the other two material

TABLE 4: Normalized principal components and DPI values.

Trial	Principal components			Normalized principal components			Grey incidence coefficient			DPI
	HV	DD	WL	HV	DD	WL	HV	DD	WL	
1	0.701	0.380	-0.106	0.000	1.000	0.247	0.333	1.000	0.399	0.495
2	1.229	-0.026	0.212	0.307	0.577	0.450	0.419	0.541	0.476	0.454
3	1.362	-0.065	0.105	0.385	0.537	0.381	0.448	0.519	0.447	0.464
4	1.021	-0.205	1.076	0.186	0.390	1.000	0.380	0.451	1.000	0.476
5	2.077	-0.418	-0.040	0.800	0.168	0.289	0.715	0.375	0.413	0.598
6	1.721	-0.292	0.178	0.593	0.299	0.428	0.552	0.416	0.466	0.510
7	1.213	0.003	0.153	0.298	0.607	0.412	0.416	0.560	0.460	0.455
8	2.420	-0.456	-0.494	1.000	0.129	0.000	1.000	0.365	0.333	0.769
9	1.933	-0.278	-0.210	0.716	0.314	0.181	0.638	0.422	0.379	0.555
10	1.428	-0.228	0.472	0.423	0.367	0.615	0.464	0.441	0.565	0.472
11	1.230	-0.061	0.312	0.308	0.540	0.513	0.419	0.521	0.507	0.454
12	2.058	-0.580	0.463	0.789	0.000	0.609	0.704	0.333	0.561	0.600
13	1.269	-0.230	0.742	0.330	0.364	0.787	0.427	0.440	0.701	0.466
14	1.769	-0.157	-0.296	0.621	0.441	0.126	0.569	0.472	0.364	0.520
15	1.091	-0.079	0.593	0.227	0.522	0.692	0.393	0.511	0.619	0.449
16	1.270	-0.138	0.470	0.331	0.460	0.614	0.428	0.481	0.564	0.457
17	1.760	-0.380	0.371	0.616	0.208	0.551	0.565	0.387	0.527	0.520
18	2.195	-0.439	-0.174	0.869	0.147	0.204	0.793	0.369	0.386	0.643

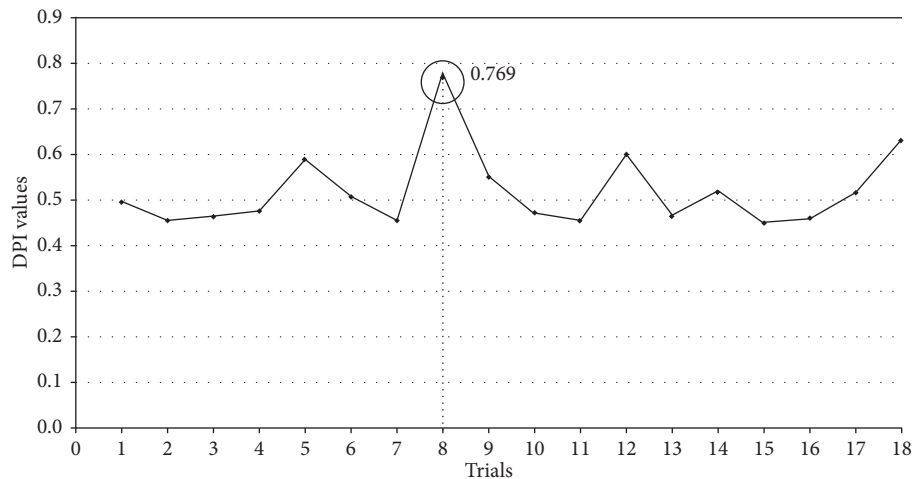


FIGURE 5: DPI values for various experimental trials.

substrates included in the study. Better diffusion depths and higher surface hardness due to interstitial diffusion of nitrogen and carbon atoms and consequent prevention of slip on a microscopic scale could be the primary reason for wear resistance in carbonitrided AISI 4140 steel (Figure 7(a)). Wear loss was observed to be better at moderate levels of carbonitriding time and ammonia flow rate as these conditions ensure a good diffusion depth and surface hardness (Figure 7(d)). Beyond a certain level, nitrogen can cause voids and porosity on the surface. Hence, nitrogen was introduced to the specimen at the end of the carburizing cycle, typically 15 min before quenching. Good hardenability in carbonitriding permits a less severe oil quench on the surface unlike pure carburizing, which requires a water quench finish [24]. Longer processing times with ammonia could result in higher levels of retained austenite and case porosity. Hence, moderate carbonitriding time was desired

for better wear resistance (Figure 7(c)). Control of carbon potential limits the solubility of carbon in the austenitic substrate, which otherwise would result in a soft deposit from carbon-enriching gas [25–29]. Furthermore, carbon diffusion limits the transformation of austenite to martensite as well [3].

4.4. Microstructure of Surface Coating. The FESEM images displaying the diffusion depths in the case of different steel substrates subjected to carbonitriding are shown in Figure 8. The interstitial diffusion of carbon and nitrogen atoms into the steel substrate produces a metallurgical surface modification and creates a barrier to slip on a microscopic scale, increasing the hardness and wear resistance [3, 22]. The coating is on a microscale with lesser distortion, permitting precise applications, which require a good degree of

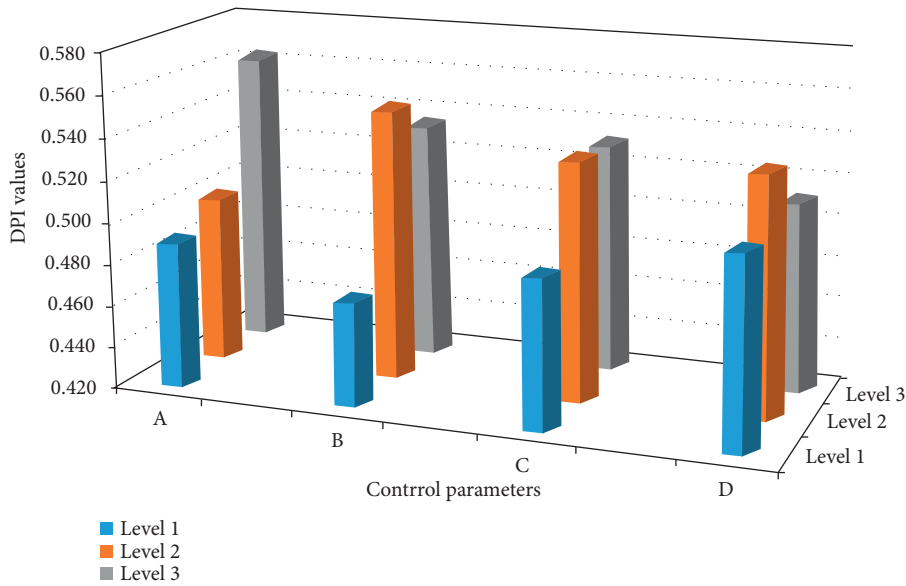
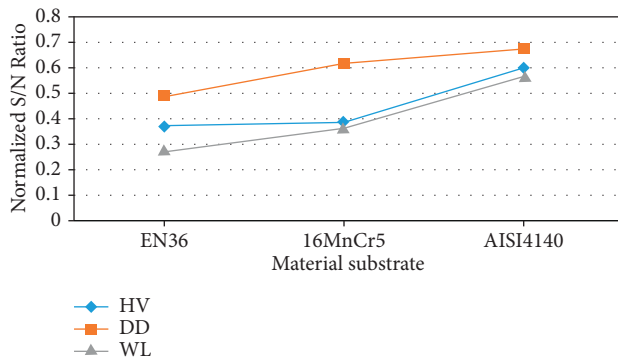


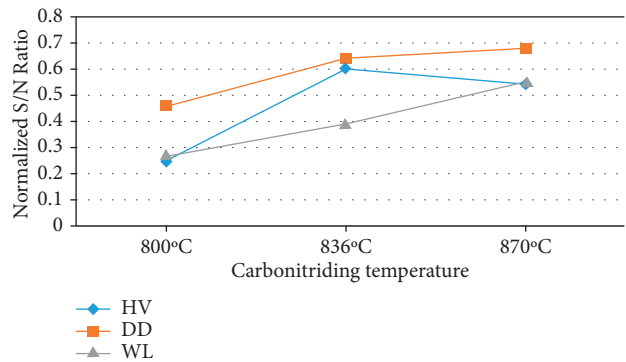
FIGURE 6: Effect of parameters on DPI.

TABLE 5: Analysis of variance on DPI values.

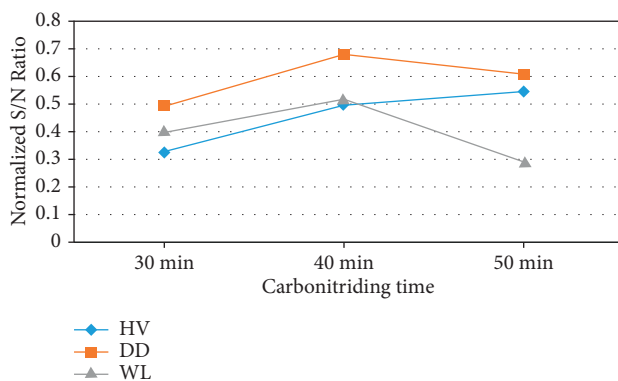
Factors	Sum of square	Degrees of freedom	Mean sum of square	F-ratio	% Contribution
A	0.0232	2	0.012	7.975	18.725
B	0.0383	2	0.019	13.184	30.953
C	0.0273	2	0.014	9.402	22.073
D	0.0219	2	0.011	7.532	17.684
Error	0.0131	9	0.001		10.565
Total	0.1238	17			100



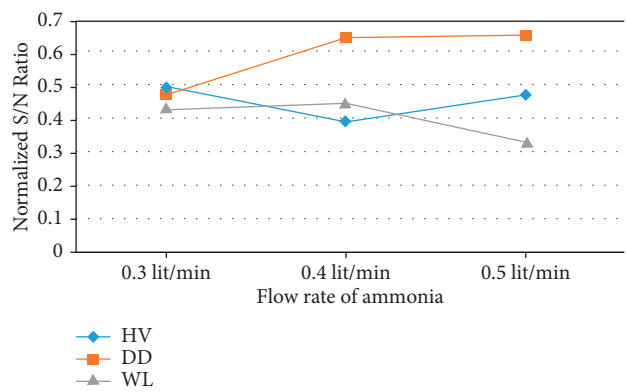
(a)



(b)



(c)



(d)

FIGURE 7: Effects of parameters on responses. (a) Material substrate. (b) Carbonitriding temperature. (c) Carbonitriding time. (d) Flow rate of ammonia.

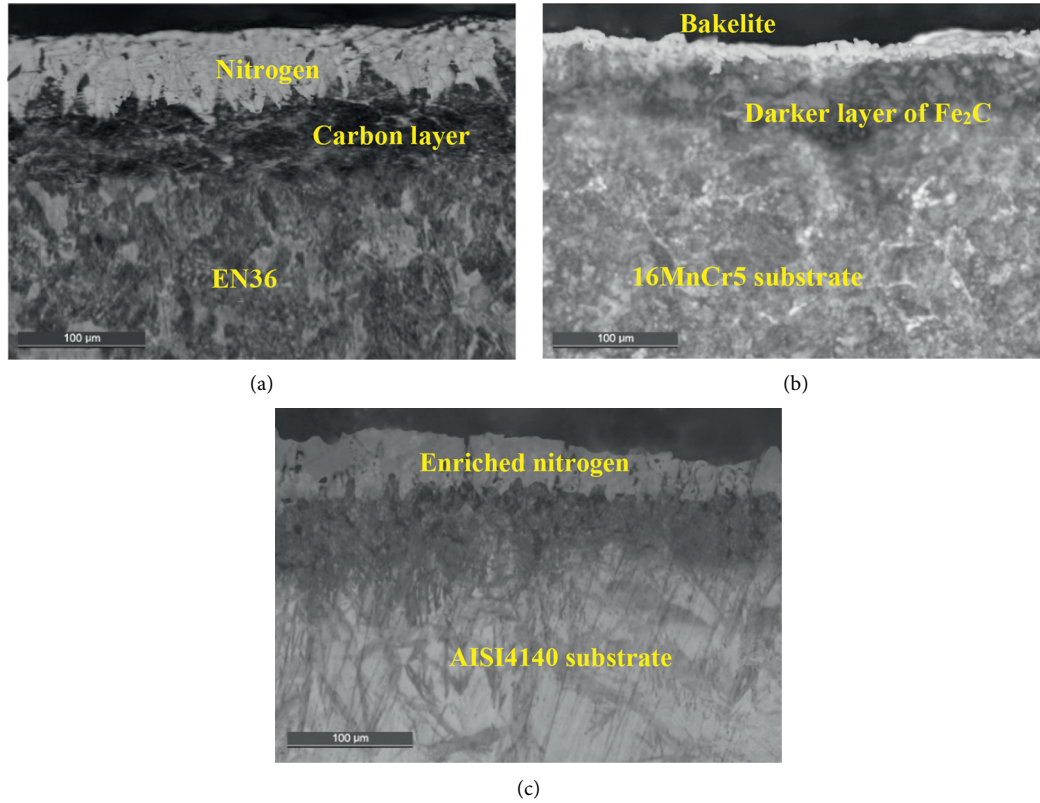


FIGURE 8: FESEM images showing diffusion depth in steel surface (a) EN36, (b) 16MnCr5, and (c) AISI 4140.

TABLE 6: Confirmation trial conducted at optimal carbonitriding condition.

Responses	Initial setting		Optimal setting using PGI method		Improvements	
	Calculated S/N ratio	Response value	Predicted S/N ratio	Response value	S/N ratio	Response value
Surface hardness (HV)	57.148	719	57.267	729	0.119	10
Diffusion depth (DD)	40.869	110	41.486	119	0.617	9
Wear loss (WL)	39.684	0.0102	41.349	0.008	1.665	0.0022
Parameter setting	$A_3 B_2 C_3 D_2$		$A_3 B_2 C_2 D_2$			

tolerance. The carbonitrided layer has an outer layer enriched in nitrogen and an internal carbon-rich layer, which is relatively darker than the outer layer. Iron carbides and iron nitrides are available in these layers along with retained austenite and fine martensite. Hence, the carbonitrided layer with precipitates of Fe_3N and Fe_2C has increased hardness, while the core is retained with the same degree of parental toughness as it is unaffected [3]. The diffusion depth in the case of carbonitrided AISI 4140 steel (Figure 8(c)) is observed to be more compared to the other two case-hardening steels (Figures 8(a) and 8(b)).

4.5. Confirmation Trial for Validation of PGI Methodology. The integrated methodology of PGI was applied to the process of surface treatment of case-hardening steels, and the optimal carbonitriding parameters producing better responses (HV, DD, and WL) were identified. Validation of results becomes essential for further applications of PGI methodology in different areas of manufacturing science. A

confirmatory trial was performed with the predicted optimal conditions (material substrate- AISI 4140, carbonitriding temperature $-835^{\circ}C$, carbonitriding time- 40 min, and flow rate of ammonia- 0.4 lit/min), and the obtained quality characteristics were compared with responses from the best experimental condition (trial 8). Good improvements were observed in responses to prove the effectiveness of the developed approach of PGI (Table 6).

5. Conclusions

A maiden attempt at the possibility of obtaining micro-surface coatings on three different grades of steels (EN36, 16MnCr5, and AISI 4140) was presented. Carbonitriding parameters were studied, and their optimal values were selected by employing a novel PGI algorithm for multi-response optimization. The methodology of PGI allows for the integration of merits of PCA and grey theory for selecting the optimal parameters inducing better surface characteristics. The following inferences were drawn.

- (i) Carbonitriding was performed on case-hardening steels (EN36, 16MnCr5, and AISI 4140), and improved surface hardness along with wear resistance was observed in all material substrates. In addition, an increased diffusion depth and surface hardness were observed in AISI 4140 steel compared to the other case-hardening steels.
- (ii) The integrated methodology of principal component-based grey incidence (PGI) had effectively predicted the optimal carbonitriding conditions (material substrate- AISI 4140 steel, carbonitriding time- 40 min, carbonitriding temperature -835°C , and flow rate of ammonia- 0.4 lit/min) for micro-surface coatings to improve the surface properties.
- (iii) The carbonitriding temperature (30.9%) and carbonitriding time (22%) were found to influence the various responses observed (surface hardness, diffusion depth, and wear loss) to a significant extent than other parameters.
- (iv) The eigenvalues and normalized principal components were used to arrive at the single entity (DPI) representing all the responses, effectively converting it into a problem of single response optimization.
- (v) The metallurgical surface modification with the outer layer of nitrogen and a relatively dark inner layer of enriched carbon were observed across the diffusion depths in all metal substrates subjected to carbonitriding. A relatively larger diffusion depth was found on the surface of AISI steel compared to the other two case-hardening steels.

The study inferences and findings can offer the necessary database for carbonitriding of case-hardening steels (EN36, 16MnCr5, and AISI 4140). This will contribute to enhancing their industrial applications in precision gears, shafts, rolled plates, strips, cam rollers, screws, and levers. This study opens up the possibility of the presentation of integrated PGI methodology in other areas of science and engineering. However, further investigations concerned with the development of sensors to maintain carbon/nitrogen potential within furnace atmosphere, along with a study of the metallurgical effects of heating-up time, will contribute to superior surface coatings. This work also opens the scope of analyzing the interaction effects of carbonitriding parameters in the near future.

Nomenclature

- η : S/N ratio.
- Y_{ij} : Response value of i th trial and j th response.
- Z_{ij} : Normalized S/N ratio value of i th trial and j th response.
- ξ : Distinctive coefficient.
- P_{mk} : Principal component values.
- Y : Grey relational coefficient.
- λ_i : Eigenvalues of i th component.
- V_{ik} : Eigenvectors of i th component.

- $\bar{\eta}$: Predicted S/N ratio.
- η_m : Average S/N ratio.

Data Availability

Data used to support the findings of this study are included within the article and are available from the corresponding author upon request.

Disclosure

This study was performed as a part of the employment at Hawassa University, Ethiopia.

Conflicts of Interest

The authors declare that there are no conflicts of interest.

Acknowledgments

The authors would wish to extend their sincere gratitude to the facilities and support offered by the Saveetha Institute of Medical and Technical Sciences, Chennai-602105, India. Industrial expertise and guidance from S.C. Atul and S.P. Chandra Sekar, Diffusion Coatech LLP and Wear cote Technologies, Tamil Nadu, India, are highly appreciated.

References

- [1] M. Li, "Practical approach to determining effective case depth of gas carburizing," *Gear Technology*, vol. 2, pp. 56–61, 2016.
- [2] C. Zheng, Y. Liu, J. Qin, R. Ji, and S. Zhang, "Experimental study on the wear behavior of HVOF sprayed nickel-based coating," *Journal of Mechanical Science and Technology*, vol. 32, no. 1, pp. 283–290, 2018.
- [3] M. Yang, H. You, and R. D. Sisson, "Nitriding and Ferritic Nitrocarburizing of Quenched and Tempered Steels," in *Proceedings of the HT2021*, pp. 110–116, ASM International, Louis, Missouri, USA, September 2021.
- [4] K.-M. Winter, "Independently controlled carbon and nitrogen potential: a new approach to carbonitriding process," *Journal of Materials Engineering and Performance*, vol. 22, no. 7, pp. 1945–1956, 2013.
- [5] E. K. Ampaw, E. K. Arthur, O. O. Adewoye, A. R. Adetunji, S. O. O. Olusunle, and W. O. Soboyejo, "Carbonitriding "pack cyaniding" of ductile irons," in *Advanced Materials Research*, vol. 1132, pp. 330–348, Trans Tech Publications Ltd, 2016.
- [6] K.-M. Winter, J. Kalucki, and D. Koshel, "Process technologies for thermochemical surface engineering," in *Thermochemical Surface Engineering of Steels*, pp. 141–206, Woodhead Publishing, 2015.
- [7] C. P. Fenili, F. S. de Souza, G. Marin, S. M. H. Probst, C. Binder, and A. N. Klein, "Corrosion resistance of low-carbon steel modified by plasma nitriding and diamond-like carbon," *Diamond and Related Materials*, vol. 80, pp. 153–161, 2017.
- [8] M. L. Fares, A. Talhi, K. Chaoui, and M. Z. Touhami, "Effects of gas carbonitriding process on surface characteristics of new hot working tool steel," *Surface Engineering*, vol. 27, no. 8, pp. 595–601, 2011.
- [9] Y. Ren, H. Wan, Y. Chen, H. Zhu, H. Lu, and X. Ren, "Effect of laser shock peening and carbonitriding on tribological

- properties of 20Cr2Mn2Mo steel alloy under dry sliding conditions,” *Surface and Coatings Technology*, vol. 417, Article ID 127215, 2021.
- [10] C. Moussa, O. Bartier, X. Hernot, G. Mauvoisin, J.-M. Collin, and G. Delattre, “Mechanical characterization of carbonitrided steel with spherical indentation using the average representative strain,” *Materials & Design*, vol. 89, pp. 1191–1198, 2016.
- [11] W. Dal’Maz Silva, J. Dulcy, J. Ghanbaja et al., “Carbonitriding of low alloy steels: mechanical and metallurgical responses,” *Materials Science and Engineering: A*, vol. 693, pp. 225–232, 2017.
- [12] L. A. Espitia, H. Dong, X.-Y. Li, C. E. Pinedo, and A. P. Tschiptschin, “Cavitation erosion resistance and wear mechanisms of active screen low temperature plasma nitrided AISI 410 martensitic stainless steel,” *Wear*, vol. 332–333, pp. 1070–1079, 2015.
- [13] C. C. Yang and C. Y. Wu, “The Optimization of Carbonitriding Process for 1022 Self-Drilling Tapping Screw with Taguchi Technique,” *International Journal of Scientific and Technical Research in Engineering (IJSTRE)*, vol. 2, no. 9, 2017.
- [14] M. Mathew and P. K. Rajendrakumar, “Optimization of process parameters of boro-carburized low carbon steel for tensile strength by Taguchi method with grey relational analysis,” *Materials & Design*, vol. 32, no. 6, pp. 3637–3644, 2011.
- [15] R. Adalarasan, M. Santhanakumar, and S. Thileepan, “Selection of optimal machining parameters in pulsed CO₂ laser cutting of Al6061/Al₂O₃ composite using Taguchi-based response surface methodology,” *International Journal of Advanced Manufacturing Technology*, vol. 93, no. 1, pp. 305–317, 2017.
- [16] M. Santhanakumar, R. Adalarasan, and M. Rajmohan, “Parameter design for cut surface characteristics in abrasive waterjet cutting of Al/SiC/Al₂O₃ composite using grey theory based RSM,” *Journal of Mechanical Science and Technology*, vol. 30, no. 1, pp. 371–379, 2016.
- [17] K. Krishnaiah and P. Shahabudeen, *Applied Design of Experiments and Taguchi Methods*, PHI Learning Pvt. Ltd, New Delhi, Delhi, 2012.
- [18] S. C. Atul, R. Adalarasan, and M. Santhanakumar, “Study on slurry paste boronizing of 410 martensitic stainless steel using taguchi based desirability analysis (TDA),” *International Journal of Manufacturing, Materials, and Mechanical Engineering*, vol. 5, no. 3, pp. 64–77, 2015.
- [19] S. C. Atul, R. Adalarasan, M. Santhanakumar, and S. C. Sekar, “Parameter design in molten salt boronizing of austenitic stainless steel using grey relational analysis,” *International Journal of Applied Engineering Research*, vol. 10, no. 33, 2015.
- [20] K. Satyanarayana, A. V. Gopal, and P. B. Babu, “Analysis for optimal decisions on turning Ti-6Al-4V with Taguchi-grey method,” *Proceedings of the Institution of Mechanical Engineers - Part C: Journal of Mechanical Engineering Science*, vol. 228, no. 1, pp. 152–157, 2014.
- [21] R. Adalarasan, M. Santhanakumar, and A. Shanmuga Sundaram, “Optimization of weld characteristics of friction welded AA 6061-AA 6351 joints using grey-principal component analysis (G-PCA),” *Journal of Mechanical Science and Technology*, vol. 28, no. 1, pp. 301–307, 2014.
- [22] J. Awrejcewicz, V. Krysko, S. Mitskievich, I. Kutepov, I. Papkova, and A. Krysko, “Principal component analysis in the linear theory of vibrations: continuous mechanical systems driven by different kinds of external noise,” *Proceedings of the Institution of Mechanical Engineers - Part C: Journal of Mechanical Engineering Science*, vol. 235, no. 1, pp. 48–62, 2021.
- [23] J. Dossett and G. E. Totten, “Introduction to surface hardening of steels,” *ASM Handbook*, vol. 4, pp. 389–398, 2013.
- [24] M. A. Kowser and M. A. Motalleb, “Effect of quenching medium on hardness of carburized low carbon steel for manufacturing of spindle used in spinning mill,” *Procedia Engineering*, vol. 105, pp. 814–820, 2015.
- [25] A. Parthiban, V. Vijayan, S. Dinesh Kumar, L. Ponraj Sankar, and N. Parthipan, “Dawit tafesse, and mebratu tufa. “Parameters of porosity and compressive strength-based optimization on reinforced aluminium from the recycled waste automobile frames,” *Advances in Materials Science and Engineering*, vol. 2021, Article ID 3648480, 10 pages, 2021.
- [26] M. Kavitha, V. M. Manickavasagam, B. Gugulothu, A. S. Kumar, S. Karthikeyan, and S. Ram, “Parameters optimization of dissimilar friction stir welding for AA7079 and AA8050 through RSM,” *Advances in Materials Science and Engineering*, vol. 2021, Article ID 9723699, 8 pages, 2021.
- [27] S. Jayaprakash, S. Siva Chandran, B. Gugulothu, R. Ramesh, M. Sudhakar, and S. Ram, “Effect of tool profile influence in dissimilar friction stir welding of aluminium alloys (AA5083 and AA7068),” *Advances in Materials Science and Engineering*, vol. 2021, Article ID 7387296, 7 pages, 2021.
- [28] V. Vijayan, A. Parthiban, L. P. Sankar, S. D. Kumar, S. Saravanakumar, and D. Tafesse, “Optimization of reinforced aluminium scraps from the automobile bumpers with nickel and magnesium Oxide in stir casting,” *Advances in Materials Science and Engineering*, vol. 2021, Article ID 3735438, 10 pages, 2021.
- [29] L. Ponraj Sankar, G. Aruna, A. Parthiban, V. Vijayan, S. Dinesh Kumar, and S. Rajkumar, “Addisalem mekonnen, and mebratu tufa. “Strength enhancement study on composites of AA6066 aluminium alloy with magnesium oxide and coal ash,” *Advances in Materials Science and Engineering*, vol. 2021, Article ID 2810106, 8 pages, 2021.